ISSN 0965-545X, Polymer Science, Series A

COMPOSITES

Enhanced Fracture Toughness and Mechanical Properties of Epoxy Resin with Rice Husk-based Nano-Silica[1]

Tien Duc Pham[a], Cuong Manh Vu[b,c,*], and Hyoung Jin Choi[d]

[a] *Faculty of Chemistry, Hanoi University of Science, Vietnam National University, Hanoi, 19 Le Thanh Tong, Hoan Kiem, Hanoi 10000, Vietnam*

[b] *Center for Advanced Chemistry, Institute of Research and Development, Duy Tan University, Da Nang, Vietnam*

[c] *Chemical Department, Le Qui Don Technical University, 236 Hoang Quoc Viet, Ha Noi, Vietnam*

[d] *Department of Polymer Science and Engineering, Inha University, Incheon 22212, Korea*

**e-mail: vumanhcuong309@gmail.com*

Received October 13, 2016;
Revised Manuscript Received December 22, 2016

Abstract—This paper reports a novel approach to toughen epoxy resin with nano-silica fabricated from rice husk using a thermal treatment method with a particle size distribution in range of 40–80 nm. The nano-silica content was in the range, 0.03–0.10 phr, with respect to epoxy. The mechanical test showed that with the addition of 0.07 phr of rice husk based nano-silica, the fracture toughness of the neat epoxy resin increased 16.3% from 0.61 to 0.71 MPa $m^{1/2}$. The dynamic mechanical analysis test results showed that the glass transition temperature (T_g) of a 0.07 phr nano-silica dispersion in epoxy resin shifted to a higher temperature from 140 to 147°C compared to neat epoxy resin. SEM further showed that the nano-silica particles dispersed throughout the epoxy resin prevented and altered the path of crack growth along with a change in the fracture surface morphology of cured epoxy resin.

DOI: 10.1134/S0965545X17030026

INTRODUCTION

In recent years, there has been increasing interest in the utilization of renewable and bio-based feedstock as advanced materials. Rice husks are one of the most abundant bio-based waste materials that are obtained from the rice-milling process with little or no commercial value, and are usually treated by burning. The main component of rice husk includes cellulose, lignin, and ash with the content dependent on the variety, climate, and geographic location of its growth [1]. Several studies have focused on the preparation of nano-silica from rice husk. Yalcin and Sevinc [2] fabricated nano-silica by an acid leaching process to remove minerals following by an alkaline leaching process using a 3% (v/v) NaOH solution for 24 h at room temperature. The pre-treated rice husk was then heat-treated at 600°C with either flowing argon or flowing oxygen. Chen et al. [1] also synthesized porous silica nanoparticles from rice husks. The applications of nano-silica from rice husk shave focused on a range of areas including the removal of organic dyes [3] and the synthesis of zeolite [4].

Epoxy resin is one of the most versatile thermosetting polymers with a wide range of industrial applications, mainly as a matrix to make composite materials in many industries, including aerospace, automotive, marine, etc. [5]. The resins, however, are inherently brittle and show poor resistance to crack propagation because of their high degree of chemical crosslinking. Therefore, epoxy toughening has long been an interesting and challenging topic in both academia and industry.

To overcome this problem, a number of approaches have been introduced. The most common methods include toughened epoxy resin (EP) using elastomers [6, 7], thermoplastics [8] or inorganic particles such as silica [9, 10], graphene [11, 12], graphene oxide [13], or using both elastomer and hard particles [14]. Vu and his team performed various studies on toughening epoxy resin [15–18], focusing on fabricated epoxy-based composite materials with high toughness. The addition of 7 phr epoxidized natural rubber (ENR), 9 phr epoxidized linseed oil (ELO), and 5 phr thiokol into the epoxy resin increased the fracture toughness significantly by 56.9, 43.1, and 80.0%, respectively, compared to the unmodified resin [15]. The use of an adduct synthesized from epoxy resin and thiokol to improve the toughness have been reported [16]. Using cellulose microfibril and poly(vinyl alcohol) nanofibers as modifiers for epoxyresin, the fracture toughness (K_{IC}) was increased 50 and 28.1%, respectively, compared to neat epoxy resin [17].

[1] The article is published in the original.

Wang et al. [19] used simultaneously carboxyl terminated butadiene acrylonitrile (CTBN) and graphene nanoplatelets (GnPs), with diameters of <1 μm (GnP-C750) and 5 μm (GnP-5), to improve the fracture toughness, mechanical, and thermal properties of composite-based epoxy resin. Their study showed that GnP-5 is more favorable for enhancing the properties of the CTBN/epoxy. GnPs/CTBN/epoxy ternary composites with significant toughness and thermal conductivity enhancements combined with comparable stiffness to that of the neat resin were achieved by incorporating 3 wt % GnP-5 into 10 wt % CTBN-modified epoxy resins.

He et al. [20] used a new family of reactive block copolymer (RBCP), poly[styrene-*alt*-(maleic anhydride)]-*block*-polystyrene-*block*-poly(*n*-butyl acrylate)-*block*-polystyrene to achieve the high fracture toughness and impact strength of epoxy. The inclusions size of RBCP in the cured blends was controlled from the nanometer to micrometer range by simply adjusting the fraction of reactive block in RBCP. These results suggest that blends containing nano inclusions of RBCP are more sensitive to the test rates. In addition, blends containing sub-micron inclusions showed substantially increased fracture toughness and IZOD impact tests without loss of transition temperature (T_g).

This paper reports the significant toughening as well as simultaneous reinforcing effects of nano-silica fabrication from rice husks on the epoxy resin. The underlying mechanism for the toughening effect was also elucidated based on morphological, mechanical, and thermomechanical studies.

EXPERIMENTAL

Materials

The epoxy resin used is based on the diglycidyl ether of bisphenol A (DGEBA, Epon 828), which was purchased from Shell Chemical and has an epoxide equivalent weight (EEW) of 185–192 g/eq. Although methyl hexahydrophthalic anhydride (MHHPA) (Lindau Chemical, England) was chosen as a curing agent, *N*-methyl imidazol (NMI) (BASF, Germany) was used as an accelerator. Scheme 1 shows the chemical structures of DGEBA, MHHPA, and NMI. Ethanol and acetone purchased from Tianjin Yongda Chemical Reagent Co. China were used as solvents. The rice husks used in this study were obtained from Huu Duc Food Commerce Co., Vietnam.

Epoxy resin

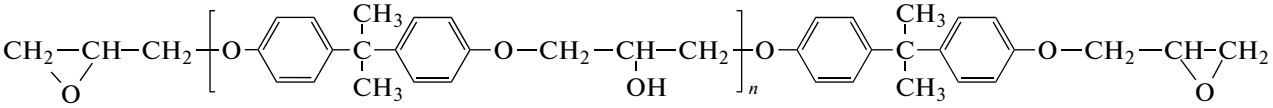

MHHPA

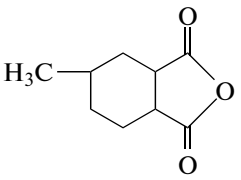

NMI

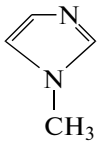

Scheme 1.

Silica Extraction from Rice Husk

In a typical experiment, 80 g of milled rice husks were placed in a beaker containing 386 g of distilled water and 14 g of sulfuric acid with stirring for 3 h at 90°C. Subsequently, the pre-treated rice husks were washed with water about four times or until all the acid had been removed. In the next step, the rice husk was dried at 100°C for 1h and calcined in a muffle furnace at 800°C for 7 h to obtain approximately 15% of the original material weight as silica. Figure 1 shows a picture of the rice husk and extracted silica, which is in the form of a white powder.

Fig. 1. (Color online) Pictures of (a) rice husk and (b) extracted nano-silica.

Composites Preparation

Nano-silica with no further modification was mixed directly into the epoxy resin with different contents (0, 0.03, 0.05, 0.07, and 0.10 phr) at 80°C for 3 h using a process homogenizer at a rotating speed of 15000 rpm. The mixture was sonicated for 15 min using an ultrasonic homogenizer. The curing agent and accelerator were added to the mixture at an EP/MHHPA/NMI molar ratio of 1/0.87/0.028, after which the mixture was degassed in a vacuum oven for 15 min. The resin mixture was then poured into a 4 mm-thick mold that was coated with a release agent. Curing was performed at 130°C for 1 h and 150°C for 1 h in a convection oven.

Measurements

For the resin fracture toughness test, all neat resin and silica-modified epoxy resin were cured at 130°C for 1 hr and then 150°C for 3 hr. The single edge notch bend (SENB) specimen was used to determine the fracture toughness (K_{IC}), as shown in Scheme 2, according to ASTM D5045-99 and was calculated from Eqs. (1) and (2).

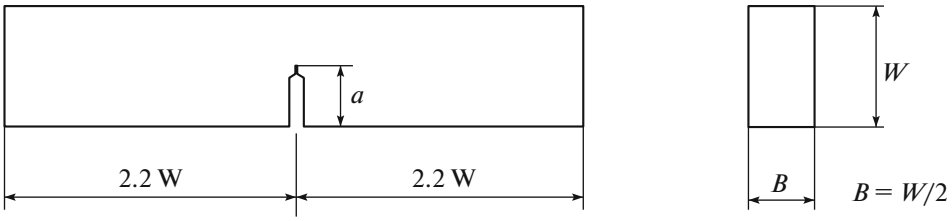

Scheme 2.

$$K_{IC} = \left(\frac{P_C}{BW^{1/2}}\right) f(x), \quad (1)$$

$$f(x) = 6x^{1/2}\frac{[1.99 - x(1-x)(2.15 - 3.93x + 2.7x^2)]}{(1+2x)(1-x)^{3/2}}, \quad (2)$$

where P_C is a critical load for crack propagation (kN), B is the specimen thickness (cm), W is the specimen width (cm), $f(x)$ is the non-dimensional shape factor, a is the crack length (cm), $x = a/W$, and $W = 2$ B. The notch tip was machined using a diamond saw. The pre-crack was generated by tapping with a fresh razor blade. After fabricating the SENB specimens, the crack tip was observed by optical microcopy, as shown in Fig. 2.

On the other hand, the tensile test of the resin was performed using the INSTRON 5582-100KN machine according to the ISO-527-1993. The specimen gauge length was 50 ± 1 mm and the testing speed was set to 2 mm/min. The specimen dimensions were 250 × 25 × 2.5 mm^3. The values were the mean of an average of five specimens. The flexural test also was performed using the INSTRON 5582-100KN machine according to the ISO 178:2010. Thermal aging of the materials with and without silica was performed according to ASTM D3045-92 (2003). The

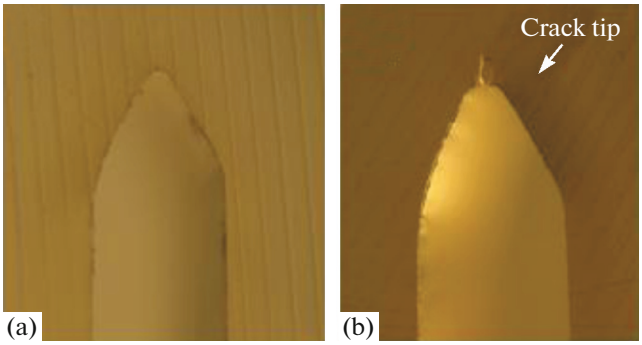

Fig. 2. (Color online) (a) The initial notch, (b) the pre-crack using a fresh razor blade.

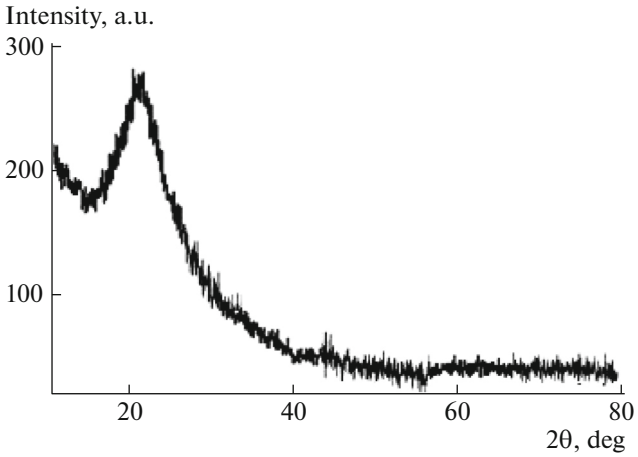

Fig. 3. XRD pattern of nano-silica particles.

samples were heated in an oven to 155°C and kept at this temperature for different ranges from 48–768 hr. After the heat induced aging process, the samples were tested and compared with the unaged sample.

For dynamic mechanical analysis (DMA) test, the DMA8000 instrument with a chuck distance of 20 mm was used to perform the DMA studies to evaluate tan δ and T_g. DMA also provides both the storage modulus and loss modulus characteristics as a function of temperature. The measurements were carried out at a heating rate of 2 grad/min from 25 to 250°C at a fixed frequency of 1 Hz in three point bending mode. The samples for DMA testing had approximate dimensions of 40 mm in length, 10 mm in width, and 2 mm in thickness. The silica nanoparticles were characterized by X-ray diffraction (XRD, Bruker D8–Advance, Germany) using CuK_α (λ = 1.54 Å) as the radiation source. The chemical structure of silica powder was determined by using FTIR (Spectrum 100, Perkin Elmer, USA).

The fractured surface of testing specimens were observed by scanning electron microscopy (SEM-JEOLJSM 6360, Japan). Prior to the SEM observations, all samples were coated a thin layer of gold to avoid electrical charging. Beside it, the specific surface area (SSA) of the prepared nano-silica powder was measured using BET surface area analyzer (Autosorb AS-1 MP, USA). The sample was degassed at 568 K for 3 h and the physi-sorption analysis was carried out with nitrogen gas as an adsorbate and liquid nitrogen as a coolant. The multi-point BET correlation technique was used to measure the SSA of the nano-silica powder.

RESULTS AND DISCUSSION

For the silica nanoparticle characteristics, the silica after fabrication from the rice husk was examined using a range of methods. Figure 3 shows XRD patterns of the silica nanoparticles obtained from rice husk. The powder XRD pattern indicated a broad peak at 2θ 22°, which revealed the amorphous nature of the silica nanoparticles. The SEM image of silica in Fig. 4 revealed a diameter in range, 40–60 nm. The SSA of the material was measured using multiple-point BET surface area analyzer. The SSA of the nano-silica powder is approximately 234.2 m^2/g (Fig. 5). BET analysis confirmed that the obtained nano silica powder is a microporous material with high SSA.

Figure 6 shows Fourier transform infrared (FTIR) spectrum of silica. The peak at 1056.2 cm^{-1} was assigned to the Si–O–Si stretch, confirming the existence of silica.

Regarding the toughness and mechanical properties, silica fabricated from the rice husk by a thermal treatment was used as a re-enforcer for the epoxy resin with no further treatment. The effects of nano-silica contents on the mechanical properties and morphology were studied in detail.

Figure 7 presents the typical tensile strength–strain curves of the samples. Figures 8a and 8b report the mean fracture tensile strength, tensile modulus, and

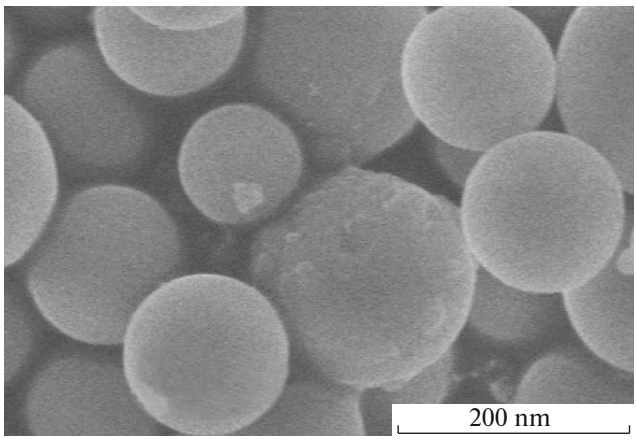

Fig. 4. SEM of nano-silica.

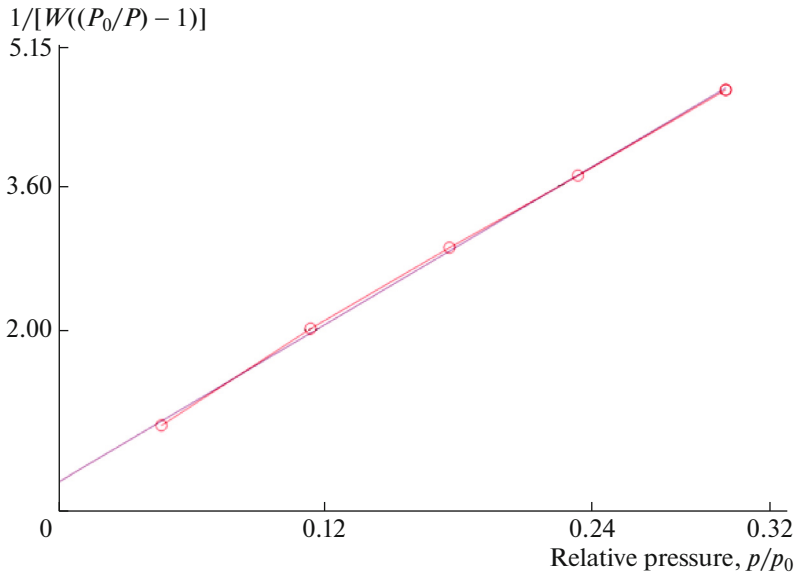

Fig. 5. (Color online) BET surface area plot of nano-silica powder.

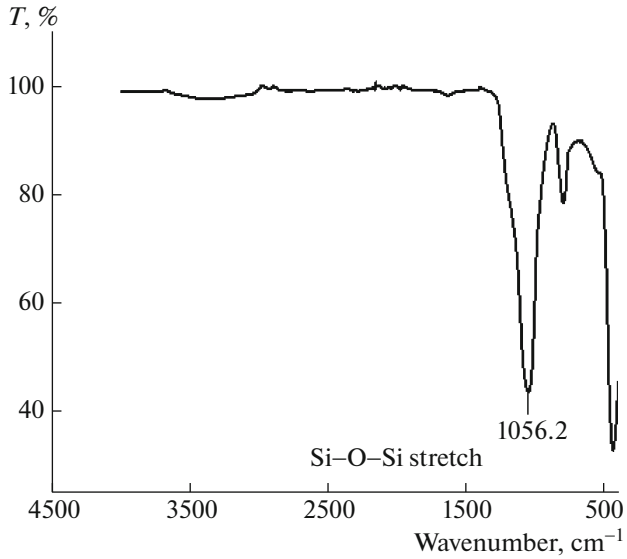

Fig. 6. FTIR of silica.

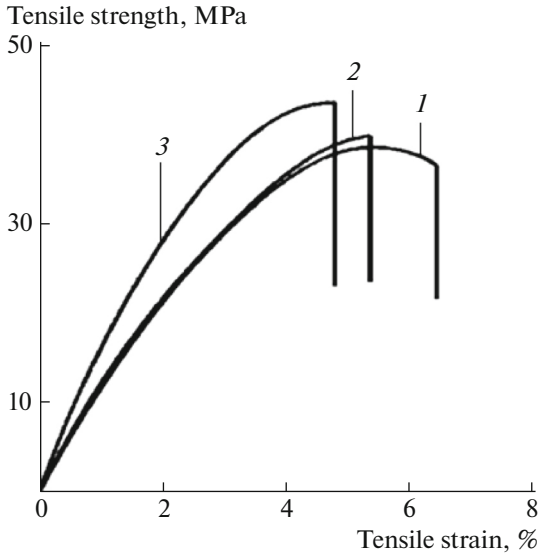

Fig. 7. Typical tensile strength–strain curves of epoxy resin were modified with (*1*) 0, (*2*) 0.03, (*3*) 0.07 phr silica.

fracture tensile strain, respectively. The introduction of nano-silica as a dispersing agent resulted in considerable enhancement of the tensile stress and tensile modulus but a decrease in tensile strain. With the dispersion of 0.07 phr nano-silica in the epoxy resin, the fracture tensile strength and modulus were increased by 7.23 and 4.37%, respectively, compared to the pure epoxy resin. On the other hand, the fracture tensile strain was decreased by 29.3%.

The fracture toughness of nano-silica–epoxy with various contents (0, 0.03, 0.05, 0.07, and 0.10 phr) was determined using the three point bending method with SENB specimens. The testing specimens were conducted at a cross–head speed of 10 mm/min, which was fast enough to prevent the viscoelastic behavior of the epoxy. The experimental results in Fig. 9 showed that the K_{IC} values of the epoxy resin were improved slightly by adding nano-silica. With the addition of 0.07 phr of nano-silica, the fracture toughness was improved by 16.3% from 0.61 to 0.71 MPa $m^{1/2}$.

Figure 10 presents the dynamic properties of the neat epoxy and its nanocomposites with 0 and 0.07 phr nano-silica. Figure 10 shows that the storage modulus

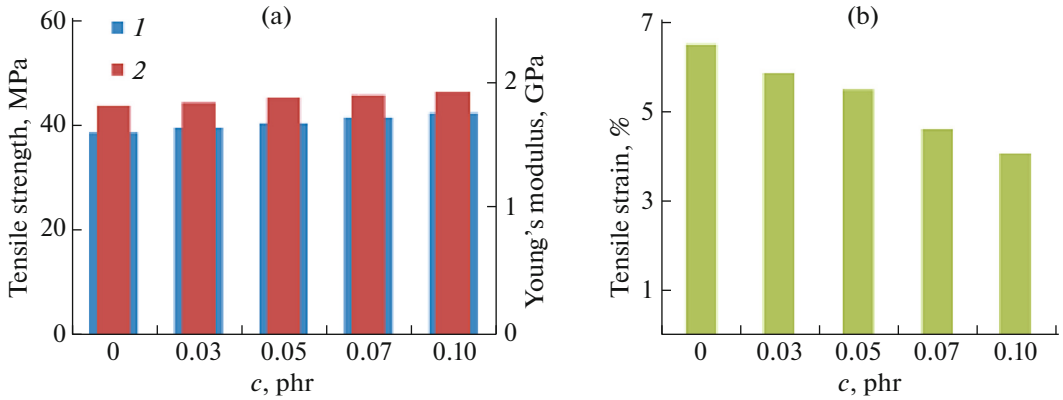

Fig. 8. (a) Comparison of (*1*) fracture tensile strength, (*2*) Young's modulus and (b) fracture strain of epoxy resin were modified with 0–0.1 phr silica as obtained from 5 sets of 6 samples for each case.

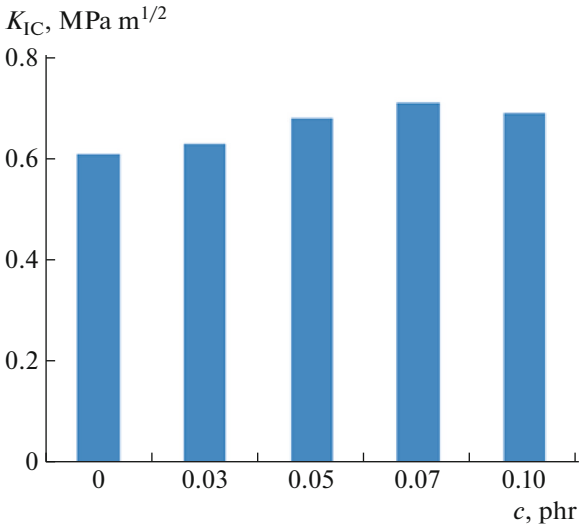

Fig. 9. Fracture toughness (K_{IC}) of the epoxy with various silica contents.

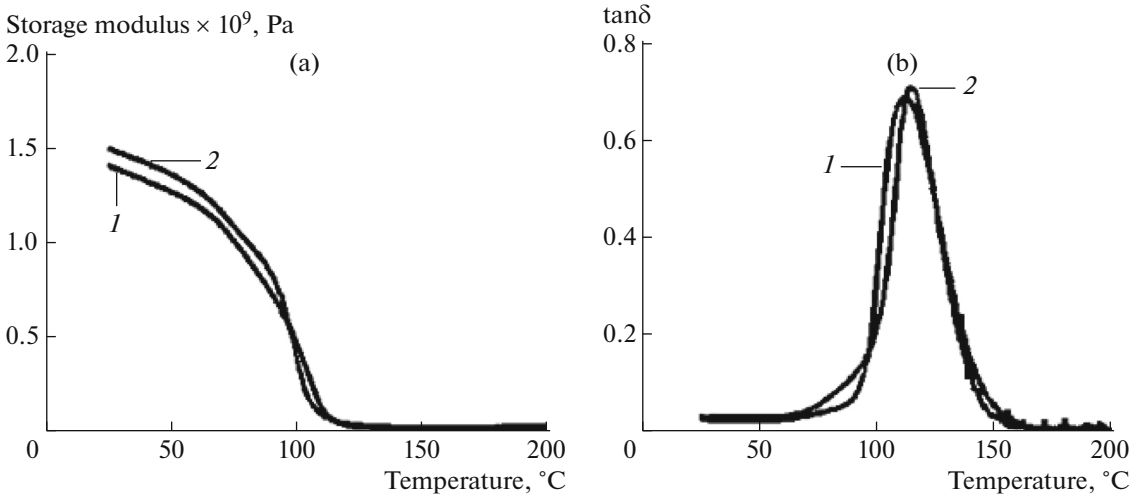

Fig. 10. (a) Loss tangent (tan δ) and (b) storage modulus versus temperature for the EP based composites with various contents of nano-silica: (*1*) 0, (*2*) 0.07 phr.

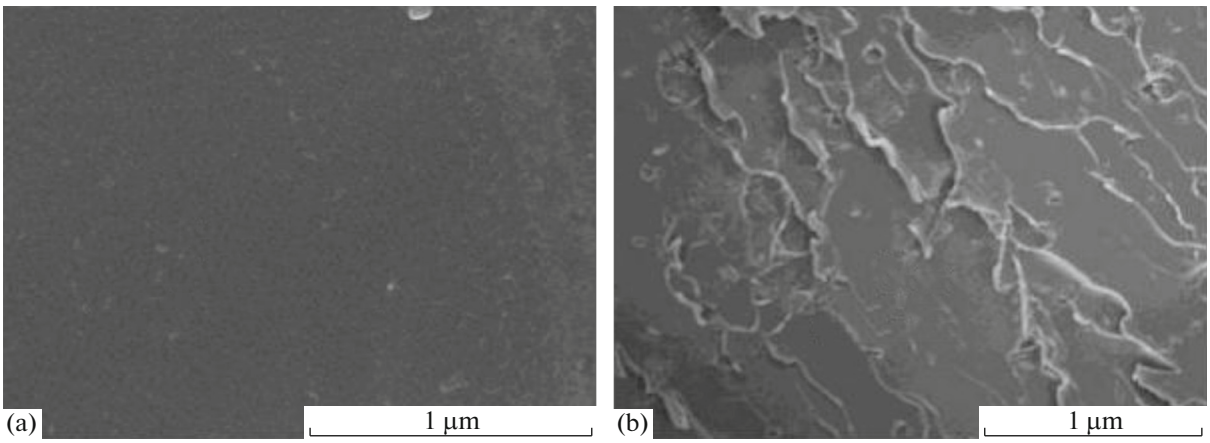

Fig. 11. SEM of fracture toughness of (a) neat epoxy resin and (b) silica modified epoxy resin.

at room temperature is increased using nano-silica. The change in storage moduli is consistent with that of the tensile moduli obtained under static testing. The above mechanical testing results highlighted the advantages of nanoparticles with a hard silica core in improving the stiffness of epoxy. This was also observed in Fig. 10 in that the glass transition temperature and the tan δ of the epoxy were increased by adding nano-silica.

Figure 11 shows the fracture surface morphology by SEM of epoxy/silica nanocomposites after fracture toughness testing. Neat epoxy exhibits a relatively smooth fracture surface (Fig. 11a), meaning that no large scale plastic deformation has occurred during the fracture process. This is agreeable with its relatively low fracture toughness. With the addition of nano-silica, the roughness fracture surface was revealed, suggesting that crack propagation could be delayed so that more energy would be required (Fig. 11b).

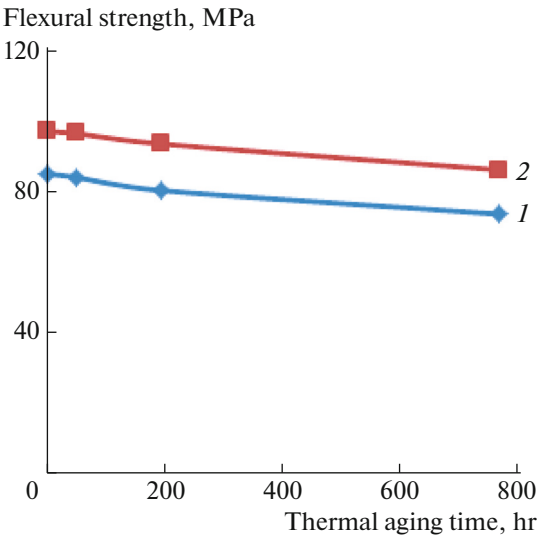

Fig. 12. Effect of thermal aging times on flexural strength of (*1*) neat epoxy resin and (*2*) epoxy resin with 0.07 phr silica.

The effects of silica on the thermal aging of epoxy resin were performed through a change in mechanical properties according to the aging time. Figure 12 shows the change in the tensile properties of epoxy resin with and without silica. Figure 12 shows that before 48 h at 155°C, there were no further changes in flexural strength. On the other hand, after 48 h at the thermal aging temperature, the change in flexural strength can be seen easily. The flexural strength of the composite based on epoxy reinforced with 0.07 phr nano-silica decreased by 0.52%, whereas the cured neat epoxy resin decreased by 1.12%. The flexural strength only decreased significantly after 192 h at the thermal aging temperature. In particular, in the composite contained 0.07 phr nano-silica, the flexural strength of the composite containing 0.07 phr nano-silica and neat epoxy resin decreased by 3.56 and 5.49%, respectively. After 768 h of thermal aging, the flexural strength of the composite containing 0.07 phr nano-silica and neat epoxy resin decreased by 11.2 and 13.43%, respectively. The decrease in flexural strength might be due to the oxidation of active groups to carbonyl groups with the incorporation of oxygen at high temperatures [21].

CONCLUSIONS

Nano-silica was prepared and incorporated into an anhydride-cured epoxy using a one-pot method. The fracture toughness of the epoxy–silica resin was improved drastically compared to neat epoxy. In particular, the sample with 0.07 phr nano-silica showed large increases of 16.3% in K_{IC} compared to that of neat epoxy. The tensile strength and Young's modulus of the epoxy–silica resin increased moderately with increasing silica loading. The toughening effect of the

silica was confirmed by microscopic SEM observations of the fracture surfaces. Overall, the effectively toughened epoxy resins with low-cost, biorenewable silica have considerable potential for use as durable coating materials or matrix materials for high performance composites.

REFERENCES

1. H. Chen, W. Wang, J. C. Martin, A. J. Oliphant, A. Doerr Pa, J. F. Xu, K. M. DeBorn, C. X. Chen, and L. Sun, ACS Sustainable Chem. Eng. **1**, 254 (2013).
2. N. Yalcin and V. Sevinc, Ceram. Int. **27**, 219 (2001).
3. G. M. K. Tolba, N. A. M. Barakat, A. M. Bastaweesy, E. A. Ashour, W. Abdelmoez, M. H. E. Newehy, and H. Y. Kim, J. Ind. Eng. Chem. **29**, 134 (2015).
4. Y. Cheng, M. Lu, J. Li, X. Su, S. Pan, C. Jiao, and M. Feng, J. Colloid Interface Sci. **369**, 388 (2012).
5. Y. Zhao, Z. K. Chen, Y. Liu, H. M. Xiao, Q. P. Feng, and S. Y. Fu, Composites, Part A **55**, 178 (2013).
6. V. D. Ramos, H. M. Costa, V. L. P. Soares, and R. S. V. Nascimento, Polym. Test. **24**, 387 (2005).
7. A. Ozturk, C. Kaynak, and T. Tincer, Eur. Polym. J. **37**, 2353 (2001).
8. X. Xie and H. Yang, Design **22**, 7 (2001).
9. T. Adachi, M. Osaki, W. Araki, and S. C. Kwon, Acta Mater. **56**, 2101 (2008).
10. S. C. Kwon, T. Adachi, W. Araki, and A. Yamaji, Composites, Part B **39**, 740 (2008).
11. S. Chandrasekaran, N. Sato, F. Tölle, R. Mülhaupt, B. Fiedler, and K. Schulte, Compos. Sci. Technol. **97**, 90 (2014).
12. D. A. Hawkins and A. Haque, Procedia Eng. **90**, 176 (2014).
13. Z. Li, R. J. Young, R. Wang, F. Yang, L. Hao, W. Jiao, and W. Liu, Polymer **54**, 582 (2013).
14. S. Sprenger, Polymer **54**, 4790 (2013).
15. C. M. Vu, L. T. Nguyen, T. V. Nguyen, and H. J. Choi, Polymer (Korea) **38**, 726 (2014).
16. C. M. Vu, L. T. Nguyen, T. V. Nguyen, and H. J. Choi, Polym. Bull. **73**, 1373 (2016).
17. C. M. Vu and H. J. Choi, Polym. Sci., Ser. A **58**, 94 (2016).
18. C. M. Vu and H. J. Choi, Polym.-Plast. Thechnol. Eng. **55** (10), 1048 (2016).
19. F. Wang, L. T. Drzal, Y. Qin, and Z. Huang, Composites, Part A **87**, 10 (2016).
20. R. He, X. Zhan, Q. Zhang, G. Zhang, and F. Chen, Polymer **92**, 222 (2016).
21. Y. Yang, G. Xian, H. Li, and L. Sui, Polym. Degrad. Stab. **118**, 111 (2015).